

# High-resolution optical coherence tomography imaging in *KCNV2* retinopathy

Panagiotis I Sergouniotis,<sup>1,2</sup> Graham E Holder,<sup>3</sup> Anthony G Robson,<sup>3</sup> Michel Michaelides,<sup>1,2</sup> Andrew R Webster,<sup>1,2</sup> Anthony T Moore<sup>1,2</sup>

<sup>1</sup>Department of Inherited Eye Disease, Moorfields Eye Hospital, London, UK

<sup>2</sup>Department of Genetics, UCL Institute of Ophthalmology, London, UK

<sup>3</sup>Electrophysiology Department, Moorfields Eye Hospital, London, UK

## Correspondence to

Professor Anthony T Moore, Moorfields Eye Hospital, 162 City Road, London EC1V 2PD, UK; [tony.moore@ucl.ac.uk](mailto:tony.moore@ucl.ac.uk)

Accepted 13 April 2011

Published Online First 10 May 2011

## ABSTRACT

**Aim** To report novel spectral domain optical coherence tomography (SD-OCT) findings and new mutational data in patients with 'cone dystrophy with supernormal rod electroretinogram', a recessive childhood onset retinal dystrophy consequent upon mutation in the *KCNV2* gene.

**Design/methods** This was a comparative case series study of 12 patients with clinical and/or electrophysiological findings in keeping with *KCNV2* mutation. Clinical examination and electrophysiological testing results were reviewed. Fundus photography and autofluorescence imaging were performed. Retinal layer appearance and thickness were evaluated using SD-OCT. The coding region and intron—exon boundaries of *KCNV2* were screened by direct sequencing.

**Results** Mutations in *KCNV2* were detected in all families; five of these changes were novel. Pattern electroretinograms were undetectable and full-field electroretinograms showed findings specific for the disorder. SD-OCT demonstrated bilateral morphological changes, usually confined to the fovea. Four foveal SD-OCT phenotypes were observed: (i) discontinuous inner and outer segment (IS/OS) junction reflectivity (6 patients), (ii) loss of IS/OS line and an optical gap in the foveola (2 patients); (iii) IS/OS junction disruption and profound foveal depth reduction, without optical gap and with preserved retinal pigment epithelium (RPE) complex (2 patients); and (iv) outer retina and RPE complex abnormalities (2 patients). Thinning of the neurosensory retina was observed in all eyes.

**Conclusion** In *KCNV2* retinopathy foveal morphological changes are evident on SD-OCT even in the early stages of disease. However, there appears to be a window of opportunity, before marked structural damage has occurred, during which novel therapeutic intervention, such as gene replacement therapy, may rescue retinal function.

## INTRODUCTION

Voltage-gated potassium channels (Kv) are transmembrane proteins that control the excitability of electrically active cells and play a fundamental role in all organs and tissues. The human genome contains 40 Kvs, which are involved in diverse physiological processes.<sup>1</sup> Each channel is formed by four  $\alpha$ -subunits, each containing six transmembrane regions clustering around a central pore. *KCNV2* encodes *Kv8.2*, a 545-amino acid Kv subunit highly expressed in the inner segments of rod and cone photoreceptors of the human retina and known to form heteromeric channels with *Kv2.1* subunits.<sup>2,3</sup>

Recessive mutations in *KCNV2* have been shown to cause a specific retinal dystrophy, 'cone dystrophy with supernormal rod electroretinogram (ERG)', which is the first disorder of the visual system to be associated with a potassium channel defect in man.<sup>3</sup> This condition was initially described in 1983 as a progressive degeneration of the cone photoreceptors associated with unique rod system abnormalities.<sup>4</sup> Patients typically present in the first 2 decades of life with reduced visual acuity, disturbance of colour vision and photophobia. Nyctalopia may also be a feature of the disorder. Affected individuals are often myopic, have a normal peripheral retinal appearance and a range of macular abnormalities on funduscopy and autofluorescence imaging.<sup>5</sup> Early diagnosis is enabled by specific electrophysiological findings. Light-adapted ERGs are usually delayed and subnormal in keeping with generalised cone system dysfunction. There is a unique rod system abnormality: dark-adapted responses to dim flashes are very delayed and subnormal but with increasing flash intensity there is disproportionate enlargement of the ERG b-wave amplitude accompanied by shortening of b-wave peak time.<sup>5,6</sup> This combination of findings has not been reported in association with any other disorder.

The detailed structural changes associated with *KCNV2* mutation have not been previously reported. The present study describes spectral domain optical coherence tomography (SD-OCT) findings in 12 patients with *KCNV2* retinopathy and reports five novel mutations.

## METHODS

### Study subjects

Twelve subjects (eight simplex cases and two sibling pairs) with clinical and/or electrophysiological examination suggestive of 'cone dystrophy with supernormal rod ERG' were ascertained in the Inherited Eye Disease Service and Electrophysiology Department of Moorfields Eye Hospital, London, UK. Eight of these cases have been partially described in earlier reports, which did not include OCT imaging or the novel mutations described herein.<sup>3,6</sup> Following informed consent, blood samples from affected individuals were collected for DNA extraction and subsequent mutation screening of *KCNV2*. The proband of one family (case 2) declined to donate blood for analysis and screening was performed with consent on parental DNA; there was consent to take part in all other aspects of the study. The study was approved by the local research ethics committee and all

investigations were conducted in accordance with the principles of the Declaration of Helsinki.

### Clinical evaluation and SD-OCT

Clinical assessment included detailed history, best corrected Snellen and/or logMAR visual acuity, dilated fundus examination, colour fundus photography, autofluorescence imaging with a confocal scanning laser ophthalmoscope and SD-OCT.

The Spectralis HRA+OCT with viewing module version 5.1.2.0 (Heidelberg Engineering, Heidelberg, Germany; 3.9  $\mu\text{m}$  axial resolution) was used to acquire tomographs. Our protocol included a horizontal, centred on the fovea, linear scan and a volume scan (19 B-scans,  $20^\circ \times 15^\circ$ ) for each eye. When subjects were unable to comply, the number of frames per B-scan was adjusted.

SD-OCT data were analysed qualitatively, with comparisons made between patients and degree of inter-ocular symmetry investigated. Central point and retinal thickness in the Early Treatment Diabetic Retinopathy Study (ETDRS) central subfield were assessed. HEYEX software interface (v 1.6.2.0; Heidelberg Engineering) was used for all measurements. Identification and evaluation of the true dimensions of the outer nuclear layer would be a better indicator of photoreceptor loss compared to global thickness, but the technique used to acquire images was not optimal for accurate segmentation and appropriate normative data are lacking.<sup>7</sup>

All subjects underwent electrophysiological assessment that included full-field ERGs and pattern ERG testing that incorporated the minimum standards of the International Society for Clinical Electrophysiology of Vision (ISCEV). The protocol also included the recording of dark-adapted ERGs to an intensity series of flashes ranging from 0.001  $\text{cd.s.m}^{-2}$  to 11.5  $\text{cd.s.m}^{-2}$  in eight increments.

### Genetic analysis

Genomic DNA was extracted from the peripheral blood lymphocytes of the donated blood samples. The *KCNV2* coding region and intron–exon boundaries of exons 1 and 2 (NM\_133497.2) were amplified and sequenced according to previously described methods.<sup>3</sup> The novel p.Thr439Ile variant was tested with 50 ethnically matched control DNAs, while the p.Ala322Pro variant was tested in 95 randomly selected, unrelated UK Caucasian blood donor DNAs (ECACC, HRC-2, Health Protection Agency Culture Collections, Salisbury, UK).

## RESULTS

### Clinical and SD-OCT findings

The clinical findings are summarised in table 1. Patients were between 13 and 48 years old and presented with reduced central vision and/or photophobia which had commenced in the first or second decade of life. Visual acuity ranged from 0.20 to 1.30 logMAR (mean 0.71). Patients 2, 5 and 8 as well as the sibling pair of 6 and 7 were born to consanguineous parents.

Pattern ERGs were undetectable in all 11 patients tested, indicating severe macular dysfunction. Full-field ERGs showed the characteristic combination of findings previously described as pathognomonic for ‘cone dystrophy with supernormal rod ERG’<sup>5, 6</sup> in all 12 patients. ERGs from patients 8 and 12 are compared with normal traces in figure 1.

Fundus autofluorescence imaging revealed abnormal macular autofluorescence in all patients. The pattern of abnormality was variable and ranged from a small perifoveal ring of increased signal (eg, case 1) to a central area of absent autofluorescence corresponding to retinal pigment epithelium (RPE) atrophy (eg, case 12) (figure 2).

SD-OCT demonstrated structural changes in all 23 eyes tested (one eye was not included in the analysis due to unstable

**Table 1** Summary of clinical findings in patients with *KCNV2* related disease

Case	Age at examination	Visual acuity*		Refraction	Ishihara colour vision test	Macular appearance on funduscopy	Autofluorescence (AF) imaging	Foveal appearance on SD-OCT
		OD	OS					
1	13	0.90	1.10	+5.00/–3.50 $\times$ 165 OD +4.50/–3.50 $\times$ 10 OS	Test plate only	Granular macular appearance	Abnormal foveal AF; small parafoveal ring of increased AF	Focal disruption of reflective band at IS/OS junction
2	13	0.90	0.75	+1.50/+1.00 $\times$ 90 OD +1.50/+1.25 $\times$ 90 OS	Test plate only	Normal	Parafoveal area of mildly increased AF	Complete loss of photoreceptor layers in the fovea
3	16	0.45	0.35	Myopic prescription	Test plate only	Subtle RPE mottling in the fovea	Parafoveal area of increased AF	Focal disruption of reflective band at IS/OS junction
4	18	0.25	0.25	Emmetropic	Test plate only	Granular macular appearance	Abnormal foveal AF; small parafoveal ring of increased AF	Focal disruption of reflective band at IS/OS junction
5	18	0.20	0.30	–8.50/–0.50 $\times$ 130 OD –7.00/–0.75 $\times$ 5 OS	Test plate only	Granular macular appearance	Parafoveal area of mildly increased AF	Focal disruption of reflective band at IS/OS junction
6	18	0.80	0.80	Emmetropic	Test plate only	Macular atrophy and flecks	Abnormal foveal AF; high density foci around the fovea	Optical gap in the fovea with absent IS/OS junction line
7	20	0.80	0.80	Emmetropic	3/17	Subtle RPE mottling in the fovea	Parafoveal area of increased AF	Small optical gap with disruption of reflective band at IS/OS junction
8	34	0.80	0.80	–12.00/–1.50 $\times$ 180 OD –12.50/–1.50 $\times$ 180 OS	Test plate only	RPE mottling in the fovea	Parafoveal area of increased AF	Focal disruption of reflective band at IS/OS junction
9	43	0.60	0.78	Emmetropic	Test plate only	Normal	Parafoveal area of increased AF	Focal disruption of reflective band at IS/OS junction
10	44	1.00	1.30	–2.75/–1.75 $\times$ 50 OD –5.50 OS	Unable to see test plate	Macular atrophy	Central loss of AF	Complete photoreceptor layers loss; RPE layer loss
11	44	0.50	0.80	–9.00/–2.00 $\times$ 180 OD –6.50/–2.00 $\times$ 5 OS	Test plate only	Subtle RPE mottling in the fovea	Central area of increased AF with surrounding area of reduced signal	Loss of photoreceptor layers in the fovea
12	48	1.00	1.00	–3.00/–2.00 $\times$ 160 OD $\infty$ /–3.00 $\times$ 30 OS	2/17	Macular atrophy	Central atrophy surrounded by ring of increased AF	Complete photoreceptor layers loss; RPE layer loss

\*LogMAR or logMAR equivalent.

IS/OS, inner segment/outer segment; OD, right eye; OS, left eye; RPE, retinal pigment epithelium; SD-OCT, spectral domain optical coherence tomography.

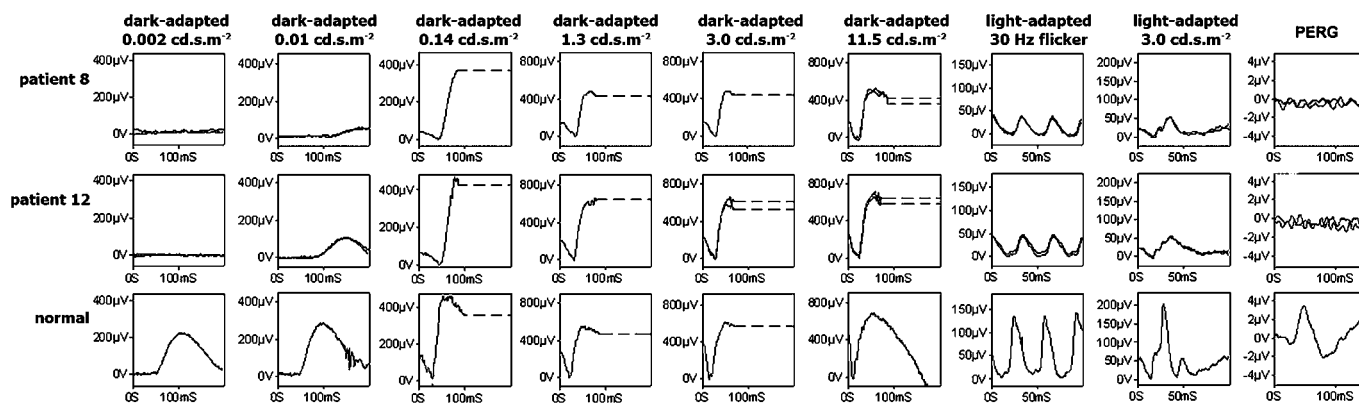


**Figure 1** Representative full field and pattern electroretinogram (ERG) traces. Patient 8 (upper row) carries biallelic nonsense mutations. Patient 12 (middle row) is homozygous for a mutation affecting the pore. The lower row shows representative normal traces. Both patients had characteristic normal findings. The dim flash ERGs ( $-3.0$  LU) are undetectable and the International Society for Clinical Electrophysiology of Vision (ISCEV) standard dark-adapted  $0.01$  ( $-2.4$  LU) shows a profoundly delayed and subnormal b-wave. With increasing stimulus intensity there is then a rapid increase in b-wave amplitude and shortening of peak time despite a relatively small increase in stimulus intensity. The brighter flash (dark-adapted  $11.5$ ;  $+0.6$  LU) ERGs show a normally developing a-wave with a broadened trough and a sharply rising high amplitude b-wave. Cone flicker (light-adapted  $30$  Hz flicker) and single flash (light-adapted  $3.0$ ) ERGs are delayed and reduced. Pattern ERGs (PERG) are undetectable.

fixation). The findings were concordant between eyes in all patients. Discontinuous reflectivity of the hyper-reflective band corresponding to the photoreceptor inner and outer segment (IS/OS) junction was the predominant feature in 11 eyes (cases 1, 3, 4, 5, 8 and 9). In four eyes (cases 6 and 7), disruption was more profound and an optical gap was seen (elsewhere described as a hyporeflective zone).<sup>8</sup> The thin reflective line corresponding to the external limiting membrane was relatively preserved in both groups. Extensive loss of IS/OS junction reflectivity with significant foveal depth reduction and a preserved RPE/Bruch's membrane complex was seen in four eyes (cases 2 and 11). RPE/Bruch's membrane band thinning was observed in addition to

the photoreceptor loss in four eyes (cases 10 and 12). Mean central point thickness (CPT) was  $141.26 \mu\text{m}$  ( $n=23$ ) and mean ETDRS central subfield thickness (CSF) was  $204.84 \mu\text{m}$  ( $n=19$ ). Both CPT and CSF were significantly reduced compared to normative data (CPT:  $227.3 \pm 23.2 \mu\text{m}$ , CSF:  $270.2 \pm 22.5 \mu\text{m}$ ), although part of this difference may be due to age, sex and axial length variability.<sup>9</sup> Peripheral outer retinal architecture was relatively well preserved on the basis of the  $20^\circ \times 15^\circ$  OCT volume scans ( $n=19$  eyes).

In terms of age, two groups can be highlighted in the present cohort. OCTs in the first group (cases 3–7, aged 16–20) demonstrated relative preservation of the external limiting

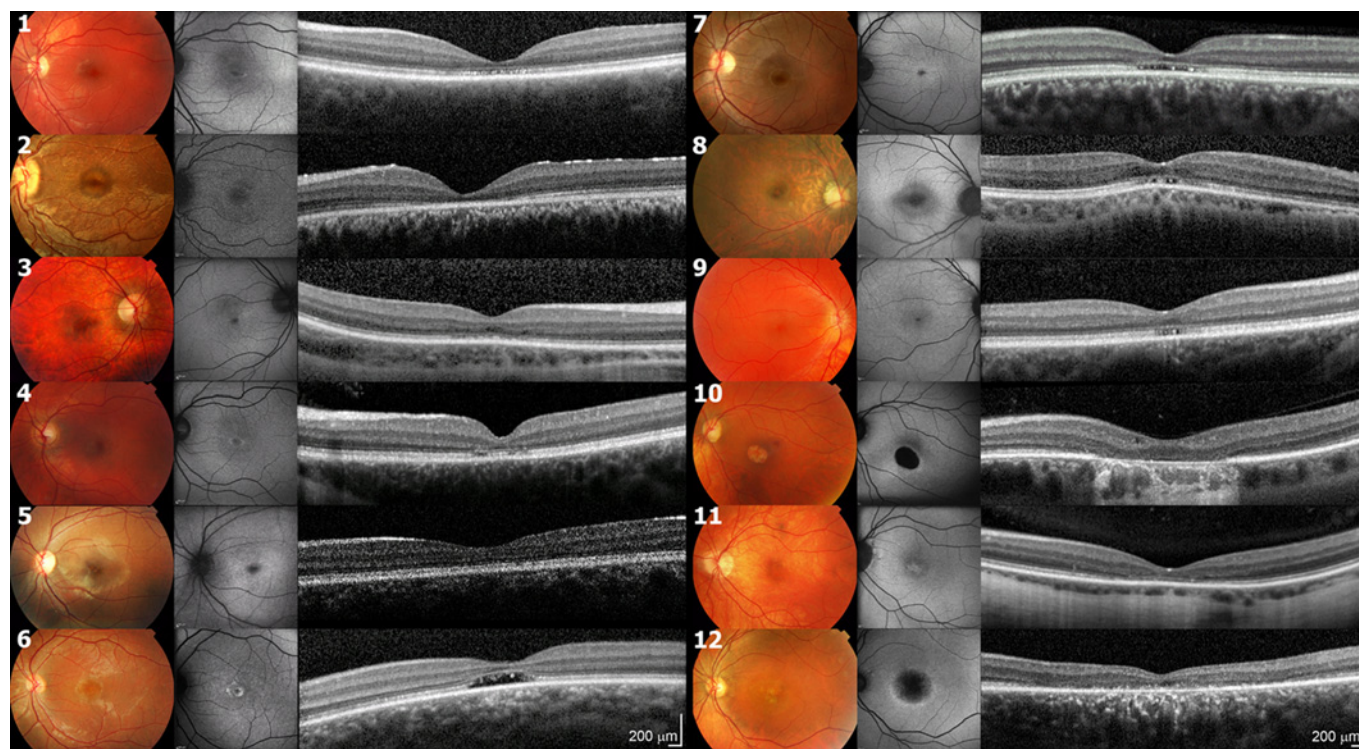


**Figure 2** Fundus photography, autofluorescence and spectral domain optical coherence tomography (SD-OCT) of 12 patients with 'cone dystrophy with supernormal rod electroretinogram' and mutations in *KCNV2*. The number relating to each triplet of images corresponds to the case number (1–12). Patients are ordered by age. SD-OCT image quality in case 5 was compromised by unstable fixation.

**Table 2** *KCNV2* mutation analysis results

Case	Mutation status	Protein domain/position	References	
			Mutation	Study subject
1	c.451T→C, p.Phe151Leu† Not identified	Cytoplasmic (NAB) Not applicable	Robson <i>et al</i> <sup>6</sup>	Case partially detailed in Robson <i>et al</i> <sup>6</sup>
2	c.427G→T, Glu143X*	Cytoplasmic (NAB)	Wu <i>et al</i> <sup>3</sup>	Previously unreported case; family members partially detailed in Wu <i>et al</i> <sup>3</sup> and Robson <i>et al</i> <sup>6</sup>
3 and 4	c.964G→C, p.Ala322Pro† c.1381G→A, p.Gly461Arg†	Transmembrane (S2) Pore (P loop)	Novel Thiagalingam <i>et al</i> <sup>11</sup>	Previously unreported cases
5	c.1318C→T, p.Thr439Ile*	Extracellular	Novel	Previously unreported case
6 and 7	c.568delG, p.Gly189fsX21*	Cytoplasmic	Novel	Cases partially detailed in Robson <i>et al</i> <sup>6</sup>
8	c.916G→T, p.Glu306X*	Transmembrane (S2)	Wu <i>et al</i> <sup>3</sup>	Case partially detailed in Wu <i>et al</i> <sup>3</sup> and Robson <i>et al</i> <sup>6</sup>
9	c.1381G→A, p.Gly461Arg† c.1637T→C, p.X546TyrX61†	Pore (P loop) Cytoplasmic (C-term)	Thiagalingam <i>et al</i> <sup>11</sup> Thiagalingam <i>et al</i> <sup>11</sup>	Case partially detailed in Robson <i>et al</i> <sup>6</sup>
10	c.430C→T, p.Gln145X† c.776C→T, p.Ala259Val†	Cytoplasmic (NAB) Extracellular (EC1)	Wu <i>et al</i> <sup>3</sup> Wu <i>et al</i> <sup>3</sup>	Case partially detailed in Wu <i>et al</i> <sup>3</sup> and Robson <i>et al</i> <sup>6</sup>
11	c.1199delT, p.Phe400fsX53† c.8_11delAACA, p.Lys3fsX93†	Cytoplasmic Cytoplasmic (N-term)	Novel Novel	Case partially detailed in Robson <i>et al</i> <sup>6</sup>
12	c.1381G→A, p.Gly461Arg*	Pore (P loop)	Thiagalingam <i>et al</i> <sup>11</sup>	Case partially detailed in Robson <i>et al</i> <sup>6</sup>

Cases 3 and 4 and cases 5 and 6 are pairs of siblings. NAB indicates the cytoplasmic domain N-terminal A and B box.

\*Homozygous state.

†Heterozygous state.

membrane and focal loss of photoreceptor outer segments. A more severe phenotype was observed in the second group (cases 9–12, aged 43–48), where there was more marked photoreceptor and/or RPE loss in three out of four patients (figure 2).

### Genetic analysis results

Either homozygous or compound heterozygous mutations were detected in nine families. Only a single heterozygous variant could be detected in one family (case 1). Five novel mutations were identified, including two missense variants: one (p.Ala322Pro) altering a not particularly conserved amino acid, located in the second transmembrane helix, and one (p.Thr439Ile) occurring at a site that is fully conserved across vertebrates and highly conserved in other Kvs, located in close proximity to the pore region (amino acids 446–463).<sup>10</sup> None of these changes was present in control chromosomes.

Three novel frameshift mutations were also identified, including two one base pair deletions and one four base pair deletion, all occurring in exon 1. In two of them (p.Lys3fsX93 and p.Gly189fsX21), mRNA would be predicted to succumb to nonsense-mediated decay; if however they were translated, the encoded proteins would be severely truncated and predicted to be non-functional since they would lack all transmembrane helices and the pore region. The p.Phe400fsX53 mutation shifts the protein frame before the fifth transmembrane domain and the pore. These results are summarised in table 2.

### DISCUSSION

This report presents novel SD-OCT data in a cohort of patients with mutations in *KCNV2* resulting in ‘cone dystrophy with supernormal rod ERG’, and describes five novel mutations. Mutations in genes encoding potassium channels cause a number of diverse phenotypes both in animal models and in man, which include long QT syndrome, epilepsy and snowflake vitreoretinal degeneration.<sup>12–14</sup> Potassium channelopathies are good candidates for novel therapeutic approaches including the development of drugs targeting the ion channel.<sup>1</sup>

SD-OCT enables high resolution, cross-sectional visualisation of retinal structure, and allows assessment of the structural integrity of the photoreceptor layer, an important parameter for the success of gene therapy or pharmacological modulation

strategies.<sup>15 16</sup> Thinning and non-specific changes in the foveal outer retinal layers were present in all patients. An unusual optical gap similar to that described in cases with achromatopsia<sup>8</sup> due to mutations in *PDE6C*<sup>17</sup> or *CNGA3*,<sup>18</sup> occult maculopathy<sup>19</sup> and less commonly in Stargardt disease,<sup>20</sup> was observed in the SD-OCTs of a sibling pair (cases 6 and 7).

In this cross-sectional study, more severe morphological changes in SD-OCT with increasing age cannot be excluded, suggesting that there might be progressive loss of foveal photoreceptors; this is consistent with observations made on the basis of autofluorescence imaging.<sup>6</sup> However, it is noted that the two youngest patients in our cohort (cases 1 and 2) presented with a relatively severe OCT phenotype and longitudinal studies are needed to more accurately determine the natural history of the disorder.

Fundoscopy and gross OCT abnormalities appear to be confined to the central retina. This is despite the fact that *KCNV2* is expressed in both rod and cone photoreceptors and the ERG changes indicate widespread retinal dysfunction. The severity of peripheral retinal dysfunction does not correlate with age and serial recordings, described in a few cases, have shown mild or no deterioration.<sup>6</sup> Colour vision testing has shown relative preservation of S-cone function.<sup>5 21</sup> These findings together with the OCT changes suggest that foveal cones are particularly susceptible to the deleterious effects of mutant *KCNV2*, or that *KCNV2* is more highly expressed in foveal cones. Future studies with cellular-resolution retinal imaging will more accurately map cone abnormalities in the foveal and parafoveal area and provide further insight.<sup>22</sup>

It has been previously highlighted that the term ‘cone dystrophy with supernormal rod ERG’ is misleading in the context of this disorder and often a misnomer.<sup>6</sup> Dark-adapted ERG amplitudes are not usually greater than normal and it is the highly abnormal intensity response function and the shape of the dark-adapted bright flash ERG that are the findings specific for the condition, together with generalised cone dysfunction (figure 2). Such findings have not been described in any other disorder. Mutations in *KCNV2* were detected in all study subjects, in agreement with previous results tightly linking the phenotype of ‘cone dystrophy with supernormal rod ERG’ with mutated *Kv8.2*.<sup>21</sup> We suggest that the term ‘*KCNV2*

retinopathy' should be used and promoted rather than 'cone dystrophy with supernormal rod ERG'.

Kv8.2 (KCNV2) subunits are not functional in isolation and do not form homomeric potassium channels. Instead, they coassemble with Kv2.1 to constitute functional heteromers.<sup>2 10</sup> Kv2.1 (KCNB1) subunits are expressed in neurons and neuroendocrine cells and can form both homo and heteromeric channels.<sup>23</sup> Mutations in *KCNV2* can lead to either completely absent or dysfunctional Kv8.2/Kv2.1 channels. When *KCNV2* mRNA is not translated, Kv2.1 homomeric channels are formed.<sup>2 24</sup> This is predicted to be the case in patients with biallelic mutations that trigger nonsense mediated mRNA decay. Conversely, mutations affecting the pore-forming loop like p.Gly461Arg are expected to result in present but non-functional Kv8.2/Kv2.1 heteromers.<sup>2 24</sup> Patients 2, 6, 7 and 8 carry alleles in the first category, while patient 12 is homozygous for a mutation in the pore. No significant difference in severity of clinical, electrophysiological (figure 1) or OCT phenotype emerges when comparing these groups with each other or with the rest of the patients.

*KCNV2* retinopathy is a recessive early onset retinal dystrophy which has a characteristic electrophysiological phenotype. Foveal structural abnormalities are demonstrated in SD-OCT even in the early stages of disease. Undetectable pattern ERG recordings are a consistent feature and suggest that there is more widespread macular dysfunction, affecting morphologically intact photoreceptors. Future therapeutic approaches such as gene replacement or pharmacological therapy may restore function to these cells or slow the degenerative process.

**Funding** The British Retinitis Pigmentosa Society, Fight for Sight, Moorfields Eye Hospital Special Trustees and the National Institute for Health Research UK provided the Biomedical Research Centre for Ophthalmology based at Moorfields Eye Hospital NHS Foundation Trust and UCL Institute of Ophthalmology, and The Foundation Fighting Blindness (USA) with funding for this study.

**Competing interests** None.

**Ethics approval** This study was conducted with the approval of the Moorfields and Whittington Hospitals Research Ethics Committee.

**Provenance and peer review** Not commissioned; externally peer reviewed.

## REFERENCES

1. Wulff H, Castle NA, Pardo LA. Voltage-gated potassium channels as therapeutic targets. *Nat Rev Drug Discov* 2009;**8**:982–1001.
2. Czirjak G, Toth ZE, Enyedi P. Characterization of the heteromeric potassium channel formed by kv2.1 and the retinal subunit kv8.2 in *Xenopus* oocytes. *J Neurophysiol* 2007;**98**:1213–22.
3. Wu H, Cowing JA, Michaelides M, et al. Mutations in the gene *KCNV2* encoding a voltage-gated potassium channel subunit cause "cone dystrophy with supernormal rod electroretinogram" in humans. *Am J Hum Genet* 2006;**79**:574–9.
4. Gouras P, Eggers HM, MacKay CJ. Cone dystrophy, nyctalopia, and supernormal rod responses. A new retinal degeneration. *Arch Ophthalmol* 1983;**101**:718–24.
5. Michaelides M, Holder GE, Webster AR, et al. A detailed phenotypic study of "cone dystrophy with supernormal rod ERG". *Br J Ophthalmol* 2005;**89**:332–9.
6. Robson AG, Webster AR, Michaelides M, et al. "Cone dystrophy with supernormal rod electroretinogram": a comprehensive genotype/phenotype study including fundus autofluorescence and extensive electrophysiology. *Retina* 2010;**30**:51–62.
7. Lujan B, Roorda A, Knighton RW, et al. Revealing Henle's Fiber Layer using Spectral Domain Optical Coherence Tomography. *Invest Ophthalmol Vis Sci* 2011;**52**:1486–92.
8. Thomas MG, Kumar A, Kohl S, et al. High-resolution in vivo imaging in achromatopsia. *Ophthalmology* 2011;**118**:882–7.
9. Grover S, Murthy RK, Brar VS, et al. Normative data for macular thickness by high-definition spectral-domain optical coherence tomography (spectralis). *Am J Ophthalmol* 2009;**148**:266–71.
10. Ottschytsch N, Raes A, Van Hoorick D, et al. Obligatory heterotetramerization of three previously uncharacterized Kv channel alpha-subunits identified in the human genome. *Proc Natl Acad Sci U S A* 2002;**99**:7986–91.
11. Thiagalingam S, McGee TL, Weleber RG, et al. Novel mutations in the *KCNV2* gene in patients with cone dystrophy and a supernormal rod electroretinogram. *Ophthalmic Genet* 2007;**28**:135–42.
12. Wang Q, Curran ME, Splawski I, et al. Positional cloning of a novel potassium channel gene: KVLQT1 mutations cause cardiac arrhythmias. *Nat Genet* 1996;**12**:17–23.
13. Biervert C, Schroeder BC, Kubisch C, et al. A potassium channel mutation in neonatal human epilepsy. *Science* 1998;**279**:403–6.
14. Hejtmancik JF, Jiao X, Li A, et al. Mutations in *KCNJ13* cause autosomal-dominant snowflake vitreoretinal degeneration. *Am J Hum Genet* 2008;**82**:174–80.
15. Jacobson SG, Aleman TS, Cideciyan AV, et al. Identifying photoreceptors in blind eyes caused by RPE65 mutations: Prerequisite for human gene therapy success. *Proc Natl Acad Sci U S A* 2005;**102**:6177–82.
16. Drexler W, Fujimoto JG. State-of-the-art retinal optical coherence tomography. *Prog Retin Eye Res* 2008;**27**:45–88.
17. Thiadens AA, den Hollander AI, Roosing S, et al. Homozygosity mapping reveals PDE6C mutations in patients with early-onset cone photoreceptor disorders. *Am J Hum Genet* 2009;**85**:240–7.
18. Thiadens AA, Somervuo V, van den Born LI, et al. Progressive loss of cones in achromatopsia: an imaging study using spectral-domain optical coherence tomography. *Invest Ophthalmol Vis Sci* 2010;**51**:5952–7.
19. Sisk RA, Berrocal AM, Lam BL. Loss of foveal cone photoreceptor outer segments in occult macular dystrophy. *Ophthalmic Surg Lasers Imaging* 9 March 2010:1–3. doi:10.3928/15428877-20100215-49.
20. Gomes NL, Greenstein VC, Carlson JN, et al. A comparison of fundus autofluorescence and retinal structure in patients with Stargardt disease. *Invest Ophthalmol Vis Sci* 2009;**50**:3953–9.
21. Wissinger B, Dangel S, Jagle H, et al. Cone dystrophy with supernormal rod response is strictly associated with mutations in *KCNV2*. *Invest Ophthalmol Vis Sci* 2008;**49**:751–7.
22. Torti C, Povazay B, Hofer B, et al. Adaptive optics optical coherence tomography at 120,000 depth scans/s for non-invasive cellular phenotyping of the living human retina. *Opt Express* 2009;**17**:19382–400.
23. Murakoshi H, Trimmer JS. Identification of the Kv2.1 K<sup>+</sup> channel as a major component of the delayed rectifier K<sup>+</sup> current in rat hippocampal neurons. *J Neurosci* 1999;**19**:1728–35.
24. Smith KE, Wilkie SE, Stocker M, et al. Cone Dystrophy With Supernormal Electroretinogram (CDSE): Functional Analysis of Mutations in *KCNV2* Encoding the Voltage-Gated Potassium Channel Subunit, Kv8.2. *ARVO Conference*. ARVO, 2010; E-Abstract 2586.



## High-resolution optical coherence tomography imaging in *KCNV2* retinopathy

Panagiotis I Sergouniotis, Graham E Holder, Anthony G Robson, Michel Michaelides, Andrew R Webster and Anthony T Moore

*Br J Ophthalmol* 2012 96: 213-217 originally published online May 10, 2011

doi: 10.1136/bjo.2011.203638

---

Updated information and services can be found at:  
<http://bjo.bmj.com/content/96/2/213>

---

	<i>These include:</i>
<b>References</b>	This article cites 22 articles, 10 of which you can access for free at: <a href="http://bjo.bmj.com/content/96/2/213#BIBL">http://bjo.bmj.com/content/96/2/213#BIBL</a>
<b>Email alerting service</b>	Receive free email alerts when new articles cite this article. Sign up in the box at the top right corner of the online article.
<b>Topic Collections</b>	Articles on similar topics can be found in the following collections <a href="#">Eye (globe)</a> (704)

---

### Notes

---

To request permissions go to:  
<http://group.bmj.com/group/rights-licensing/permissions>

To order reprints go to:  
<http://journals.bmj.com/cgi/reprintform>

To subscribe to BMJ go to:  
<http://group.bmj.com/subscribe/>